Science Bulletin 67 (2022) 38–44

Contents lists available at ScienceDirect

Science Bulletin

journal homepage: www.elsevier.com/locate/scib

Article

Field-tuned quantum effects in a triangular-lattice Ising magnet

Yayuan Qin [a,1], Yao Shen [a,b,1], Changle Liu [a], Hongliang Wo [a,c], Yonghao Gao [a], Yu Feng [d,e,f], Xiaowen Zhang [a], Gaofeng Ding [a,c], Yiqing Gu [a,c], Qisi Wang [a,g], Shoudong Shen [a], Helen C. Walker [h], Robert Bewley [h], Jianhui Xu [i,2], Martin Boehm [j], Paul Steffens [j], Seiko Ohira-Kawamura [f], Naoki Murai [f], Astrid Schneidewind [k], Xin Tong [d,e], Gang Chen [a,l,o,*], Jun Zhao [a,c,m,n,o,*]

[a] State Key Laboratory of Surface Physics and Department of Physics, Fudan University, Shanghai 200433, China
[b] Condensed Matter Physics and Materials Science Department, Brookhaven National Laboratory, Upton, New York 11973, USA
[c] Shanghai Qizhi Institute, Shanghai 200232, China
[d] Institute of High Energy Physics, Chinese Academy of Sciences (CAS), Beijing 100049, China
[e] Spallation Neutron Source Science Center, Dongguan 523803, China
[f] Materials and Life Science Division, J-PARC Center, Tokai, Ibaraki 319-1195, Japan
[g] Physik-Institut, Universität Zürich, Zürich CH-8057, Switzerland
[h] ISIS Facility, Rutherford Appleton Laboratory, STFC, Chilton, Didcot, Oxon OX11 0QX, UK
[i] Helmholtz-Zentrum Berlin für Materialien und Energie GmbH, Berlin D-14109, Germany
[j] Institut Laue-Langevin, Grenoble 9, Cedex 38042, France
[k] Jülich Centre for Neutron Science (JCNS) at Heinz Maier-Leibnitz Zentrum (MLZ), Forschungszentrum Jülich GmbH, Garching 85748, Germany
[l] Department of Physics and HKU-UCAS Joint Institute for Theoretical and Computational Physics at Hong Kong, The University of Hong Kong, Hong Kong, China
[m] Institute of Nanoelectronics and Quantum Computing, Fudan University, Shanghai 200433, China
[n] Shanghai Research Center for Quantum Sciences, Shanghai 201315, China
[o] Collaborative Innovation Center of Advanced Microstructures, Nanjing University, Nanjing 210093, China

ARTICLE INFO

Article history:
Received 19 April 2021
Received in revised form 17 June 2021
Accepted 13 August 2021
Available online 25 August 2021

Keywords:
Neutron scattering
Quantum magnet
Magnetic frustration
Transverse field Ising model

ABSTRACT

We report thermodynamic and neutron scattering measurements of the triangular-lattice quantum Ising magnet $TmMgGaO_4$ in longitudinal magnetic fields. Our experiments reveal a quasi-plateau state induced by quantum fluctuations. This state exhibits an unconventional non-monotonic field and temperature dependence of the magnetic order and excitation gap. In the high field regime where the quantum fluctuations are largely suppressed, we observed a disordered state with coherent magnon-like excitations despite the suppression of the spin excitation intensity. Through detailed semi-classical calculations, we are able to understand these behaviors quantitatively from the subtle competition between quantum fluctuations and frustrated Ising interactions.

1. Introduction

Ising model is a stereotype model in modern statistical physics and has revolutionarily advanced our understanding of phase transitions [1]. It can be realized in quantum magnets with a strong easy-axis anisotropy that pins the spin moments towards a fixed axis. Due to the pinning effect, the quantum effect is suppressed, and the physics becomes rather classical [2]. To introduce quantum effects, one usually applies an external magnetic field along the transverse direction and creates a quantum Ising model [3–7]. Representative examples of this type include the quasi-one-dimensional magnets $CoNb_2O_6$ (Ref. [8]), $BaCo_2V_2O_8$ (Refs. [9–11]), and $SrCo_2V_2O_8$ (Refs. [12,13]), in which quantum criticality and novel transitions have been reported. Nevertheless, the experimental realization of quantum Ising model in two dimensional systems is rare despite decades of theoretical efforts [4,14–18]. In contrast to this conventional route, nature provides a distinct example of quantum Ising magnets that build quantum mechanics intrinsically in the system. The observation is that, although the exchange interaction is primarily Ising like, the intrinsic crystal electric field (CEF) splitting of the Ising moment naturally creates quantum effects out of these classically interacting degrees of freedom [19–21]. These systems are quoted as "intrinsic quantum Ising magnets".

* Corresponding authors.
E-mail addresses: gangchen.physics@gmail.com (G. Chen), zhaoj@fudan.edu.cn (J. Zhao).
[1] These authors contributed equally to this work.
[2] Current address: Heinz Maier-Leibnitz Zentrum (MLZ), Technische Universität München, Garching 85748, Germany.

https://doi.org/10.1016/j.scib.2021.08.012
2095-9273/

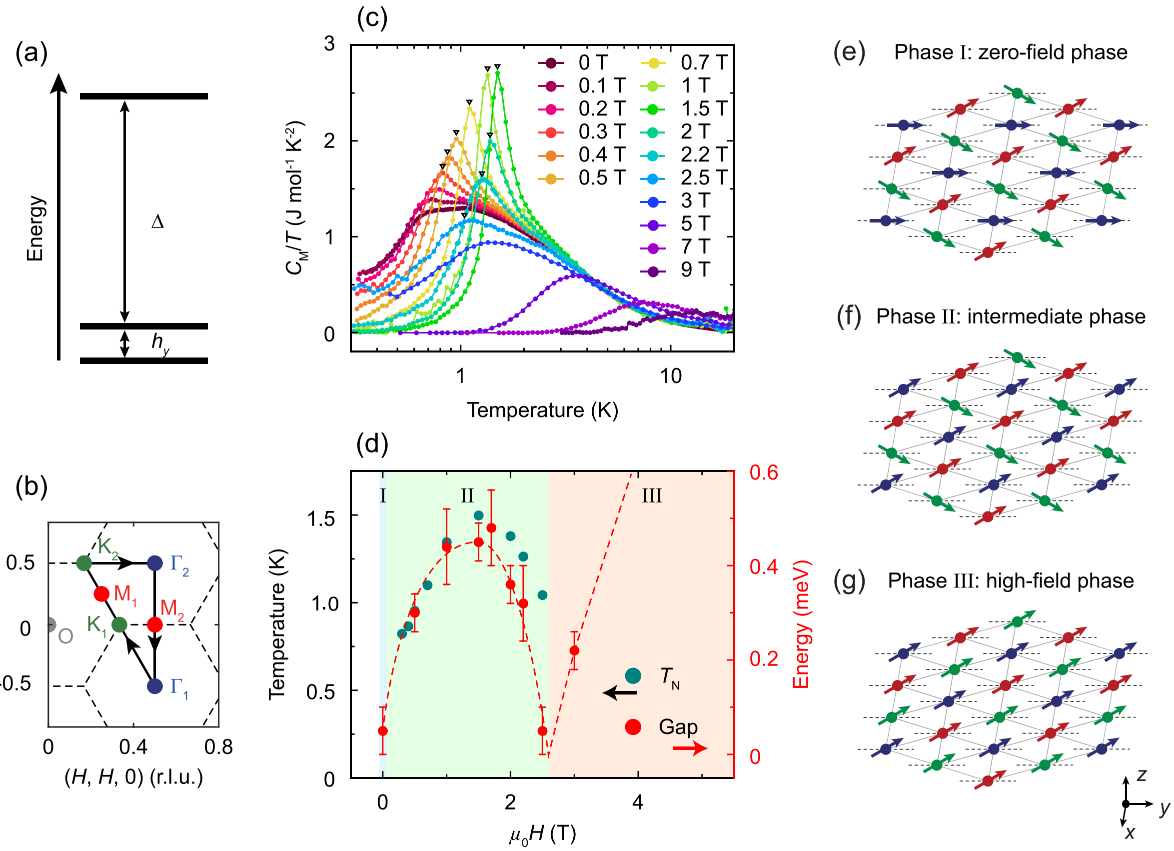

Fig. 1. (Color online) Heat capacity and magnetic phase diagram of $TmMgGaO_4$. (a) Schematic of the low energy CEF levels of Tm^{3+} ions in $TmMgGaO_4$. The ground-state quasi-doublet is well separated from the high-energy excited state ($\Delta \sim 38$ meV), indicating an effective spin-1/2 state at low temperature [23,29]. (b) Sketch of the reciprocal space in *xy* plane. The dashed lines denote Brillouin zone boundaries and the wavevector is defined as $\mathbf{Q} = H\mathbf{a}^* + K\mathbf{b}^* + L\mathbf{c}^*$; r.l.u., reciprocal lattice unit. (c) Magnetic heat capacity in various longitudinal fields ($H \| z$). The phonon contributions were subtracted by measuring the non-magnetic iso-structural $LuMgGaO_4$ single crystal. The transition temperatures are marked by black triangles. (d) Magnetic phase diagram consisting of field dependent T_N determined from heat capacity, and spin gaps at K points determined from INS data below 0.15 K. The phase diagram can be divided into three parts. Phase I: zero-field phase; Phase II: intermediate phase; Phase III: high-field phase. The dashed line is a guide to the eye. (e)–(g) Schematics of the semi-classical spin structures regarding the three phases in (d). The dashed lines denote the virtual *y* direction and different colors indicate three different sublattices.

The triangular-lattice antiferromagnet $TmMgGaO_4$ (Ref. [22]) is a promising candidate for such requirements. Due to the strong spin–orbit coupling (SOC) and CEF splitting, the CEF ground state wave function of Tm^{3+} ions is dominated by $J^z = \pm 6$, leading to a large magnetic moment of 6.59 μ_B/Tm^{3+} and Ising spin nature [23]. Thus, quantum effects are expected to be significantly suppressed. Interestingly, however, the $TmMgGaO_4$ CEF ground state is a quasi-doublet composed of two singlets separated by a small energy gap that can be mapped into an effective transverse field h_y (Fig. 1a). In this case, the transverse field, which is intrinsic in origin and homogeneous in general, leads to quantum tunneling effects among various Ising spin configurations and strongly competes with the Ising-type interactions [19–21]. Different from the coherent quantum fluctuations in quantum spin liquids that lead to long-range entanglement [24–27], the quantum effects here are of single-ion level and will potentially stabilize three-sublattice ordering. Meanwhile, short-range quantum entanglement emerges from the non-commutativeness between transverse field and Ising interactions, which may renormalize the magnetic interactions. The magnetic properties can be effectively described by the transverse field Ising model (TFIM) [23,28]

$$\mathcal{H} = \sum_{ij} J_{ij}^{zz} S_i^z S_j^z - \sum_i (h_y S_i^y + B_z S_i^z), \tag{1}$$

where the Ising exchange interactions can be kept within the first few neighbors and are geometrically frustrated. Intriguingly, due to the large *g*-factor in $TmMgGaO_4$ ($g_\| \sim 13.18$) [29], the contribution from external longitudinal field, $B_z = g_\| \mu_B B$, is comparable to the Ising interactions and quantum fluctuations so that the interplay between quantum and classical contributions can be easily tuned by external field. Therefore, $TmMgGaO_4$ provides a unique platform to manipulate the quantum effects in a controlled manner.

Moreover, in rare-earth materials, due to the complex SOC and CEF splitting, the pseudo-spins can host multipolar behaviors [30–32]. In the case of $TmMgGaO_4$, we find that the transverse components of the pseudo-spins, S^x and S^y, behave as multipoles that cannot be directly detected by neutron diffraction while the longitudinal one, S^z, remains dipolar. Its zero-field magnetic ground state is an intertwined dipolar and multipolar order in which the dipolar S^z forms a three-sublattice clock phase and the multipolar S^x/S^y components are ferro-aligned [23,28]. The observed spin excitations are in a reasonable agreement with the linear spin wave (LSW) theory, in which, however, only S_{zz} channel is detectable, arising from the coherent spin wave excitations and fluctuations of the multipolar components [32,33]. In this paper, we continue this research and study the evolution of intrinsic quantum properties of $TmMgGaO_4$ in longitudinal fields.

2. Results

2.1. Heat capacity and neutron diffraction

We start by reviewing the phase transitions of $TmMgGaO_4$ in absence of external field. Although no λ-shaped transition is pre-

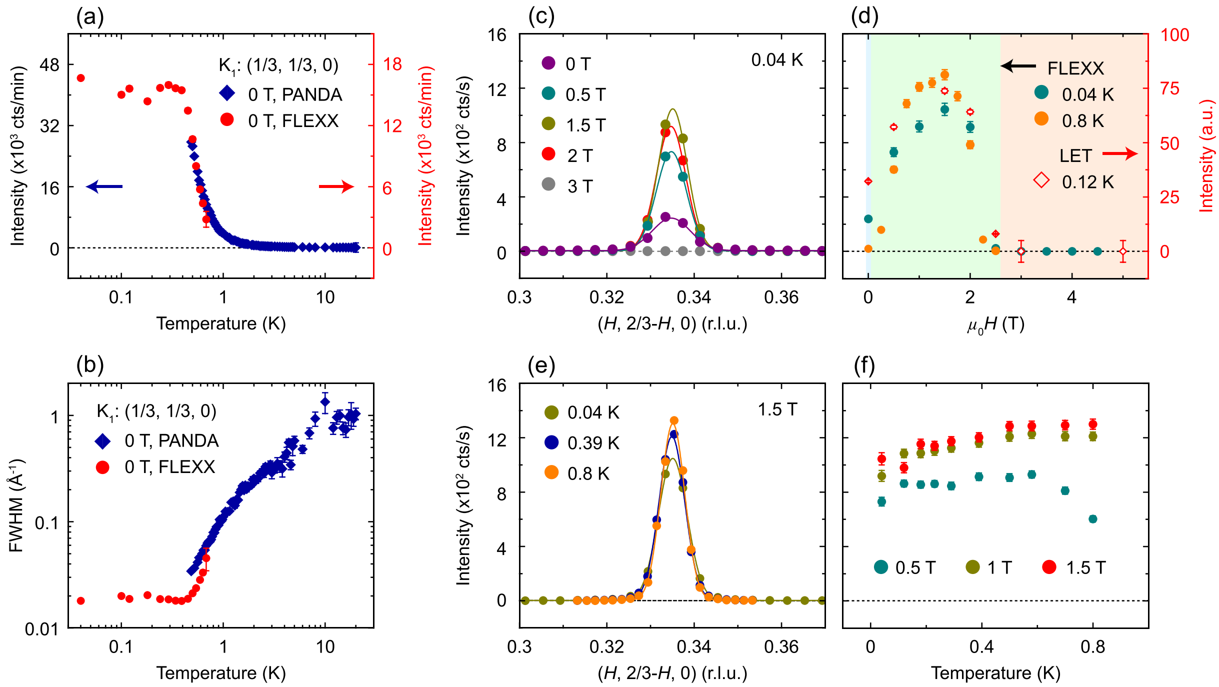

Fig. 2. (Color online) Neutron diffraction data as a function of field and temperature. (a), (b) Temperature dependence of the peak intensities and full-width at half-maximum (FWHM) of the magnetic Bragg peak at K_1 point. (c) Qscans near the magnetic peak, **Q** = (1/3, 1/3, 0), in different longitudinal fields. (d) Field dependence of the fitted amplitude of the magnetic peaks at different temperatures. (e) Representative Qscans near the magnetic peak at different temperatures in external field of 1.5 T. (f) Temperature dependence of the fitted peak amplitude at **Q** = (1/3, 1/3, 0) in different fields. The solid lines in (c) and (e) are the fitting results with Gaussian profiles and a flat background, which are also used to evaluate the peak intensities and FWHM in (a), (b), (d) and (f). Data in (c), (e) and (f) are collected at FLEXX spectrometer. a.u., arbitrary unit; cts/s, counts per second; cts/min, counts per minute; error bars, 1 s.d.

sent in the heat capacity data (Fig. 1c), well-defined magnetic Bragg peak associated with the three-sublattice spin order is observed at the K point, **Q** = (1/3, 1/3, 0), at low temperature (Fig. 2c). With temperature decreasing from 20 K, the intensity gradually increases with reduced peak width (Fig. 2a, b). The most abrupt change takes place around 1 K, which corresponds to a shoulder-like anomaly in the heat capacity (Fig. 1c). Both the peak intensity and peak width saturate below ~0.4 K. When a small magnetic field is applied along the longitudinal z direction, the heat capacity shows a sharp anomaly, indicating a new magnetic phase transition (Fig. 1c). The transition temperature, T_N, increases with increasing field, reaches a maximum at ~1.5 T, and then decreases with further increasing field (Fig. 1d). The transition completely vanishes above ~2.7 T.

To elucidate the nature of the phase transitions in longitudinal fields, we performed neutron diffraction measurements at various temperatures. As shown in Fig. 2c, d, the magnetic Bragg peak intensity at K point with temperatures of 0.04, 0.12 and 0.8 K also shows a maximum around 1.5 T, and disappears at ~2.7 T. This indicates that the phase transition seen in heat capacity measurements is also associated with the K point order. Moreover, the peak intensities in magnetic fields of 0.5, 1, and 1.5 T are enhanced in the intermediate temperature range ($0.2 \lesssim T \lesssim 0.8$ K) below T_N, distinct from a conventional order parameter behavior (Fig. 2e, f). The unusual enhancement of the magnetic peak on warming is due to the competition between thermal and quantum fluctuations, as will be discussed subsequently.

2.2. Inelastic neutron scattering

The enhancement of magnetic order in longitudinal fields has been interpreted either as the consequence of quantum fluctuations in TFIM [28], or large CEF randomness induced by structural disorder [29]. To further distinguish these two scenarios, we used inelastic neutron scattering (INS) to measure the detailed field dependence of the spin excitations in $TmMgGaO_4$. Fig. 3a–e exhibit a series of neutron spectra along the high symmetry directions in various fields. Compared with the zero-field data in Fig. 3a, the overall spin excitations in external field of 1.5 T tend to shift towards higher energies, leading to an enlarged spin gap (Fig. 3b). This is clearly inconsistent with the CEF randomness picture in which it was suggested that the system would be gapless in external field [29]. Instead, it can be readily understood without introducing much structural disorder. Below 1.5 T, the spin gap increases with increasing field (Fig. 1d). Thus, the system needs more energy to excite the quasi-particles from the magnetic ground state, implying a more stable order. Consequently, the magnetic Bragg peaks at K points are getting stronger and T_N is higher. Above 1.5 T, the spin gap gradually decreases with field and both the magnetic peak intensity and T_N are reduced (Figs. 1d, 2d). When the external field goes across the transition of ~2.7 T into the high-field regime, the spin gap reappears, indicating that the external field overcomes the spin–spin correlations and the Zeeman term dominates the spin dynamics, making the excitations less dispersive (Fig. 3e). The relatively sharp excitations observed in various fields suggest that the structural disorder is not significant in $TmMgGaO_4$.

The Ising interactions arise from the exchange and dipole–dipole interactions among Tm^{3+} local moments. For a classical Ising model, the excitations correspond to Ising spin flipping and are non-dispersive. In $TmMgGaO_4$, due to the presence of intrinsic transverse field, the excitations become dispersive. To further determine the nature of the spin excitations, we carried out polarized neutron scattering measurements on $TmMgGaO_4$. It is shown that the spin excitations are essentially longitudinally polarized in the S_{zz} channel while the transverse S_{+-} component is absent (Fig. 4a) (Supplementary materials). This is completely different from the classical spin wave with only transverse excitations at

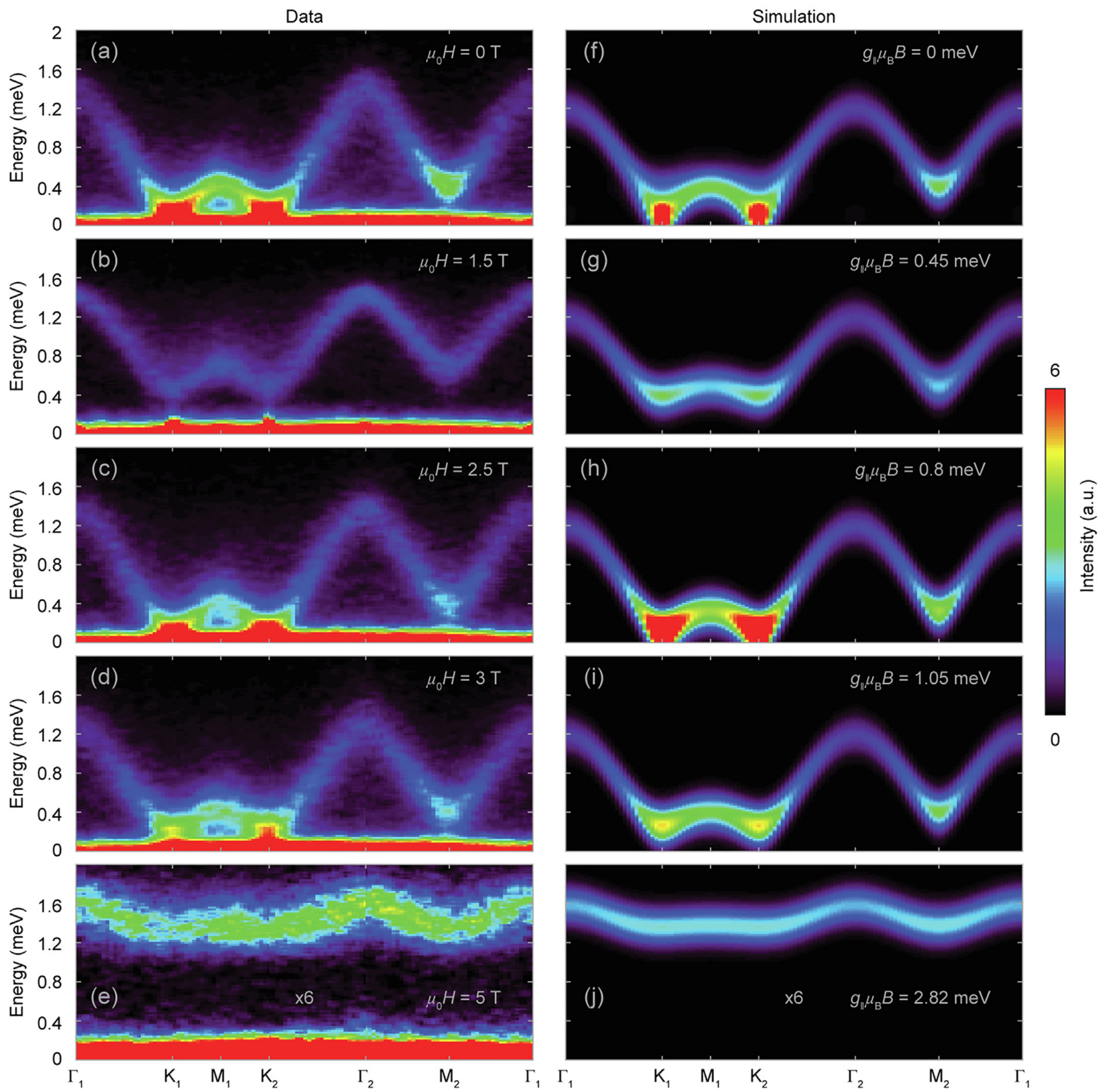

Fig. 3. (Color online) Spin excitations in different longitudinal fields at 0.12 K. (a)–(e) INS spectra of the spin excitations in $TmMgGaO_4$ along the high symmetry directions marked by the black arrows in Fig. 1b in the indicated fields. (f)–(j) Calculated spin wave dispersions using the model specified in the main text. Intensities in (e) and (j) are multiplied by 6. The intensity scale for the inelastic spectra is uniform throughout the text.

low energies. Therefore, the longitudinal channel of INS spectra, S_{zz}, manifests the quantumness of the excitations that are strictly forbidden for classical spins.

2.3. Phase diagram

After confirming the quantum fluctuations in $TmMgGaO_4$, we can understand the phase diagram comprehensively. Due to the single-ion quantum fluctuations, the dressed Ising moments are no longer homogeneous but modulated from site to site, the order of which resembles the spin density wave in quantum spin chains [34]. In zero field, the competition between classical Ising interactions and quantum fluctuations drives the system into a three-sublattice phase with up–down-zero configuration in each triangle (Phase I in Fig. 1d). The quantum fluctuation in this phase is so strong that the magnetic moments are significantly reduced. In weak longitudinal fields, the classical triangular-lattice Ising magnet would evolve into a two-up-one-down 1/3-plateau state [35–39]. In $TmMgGaO_4$, the quantum fluctuations turn it into a quasi-plateau phase with modulated spin moments (Phase II). Here, the external field acts as an extra classical contribution and suppresses the quantum effects. As a result, the magnetic order is enhanced with stronger magnetic peaks at K points, higher T_N and a larger spin gap. Since the spin dynamics here are of quantum origin, the INS intensity is weaker (Fig. 4b, c). Moreover, at higher temperatures, the quantum effects are partially quenched due to the thermal fluctuations, leading to enhanced magnetic Bragg peaks at higher temperatures (Fig. 2e, f). When the field is further increased towards the transition field $\mu_0 H_c \sim 2.7$ T, the quantum fluctuation is enhanced again and the rebuilt quantum effects suppress the static magnetic order, reduce the spin gap and lower the transition temperature while the quantum excitations grow in intensity (Figs. 1d, 4b, 4c). Above $\mu_0 H_c$, the three-sublattice magnetic order is completely eliminated and the system enters the

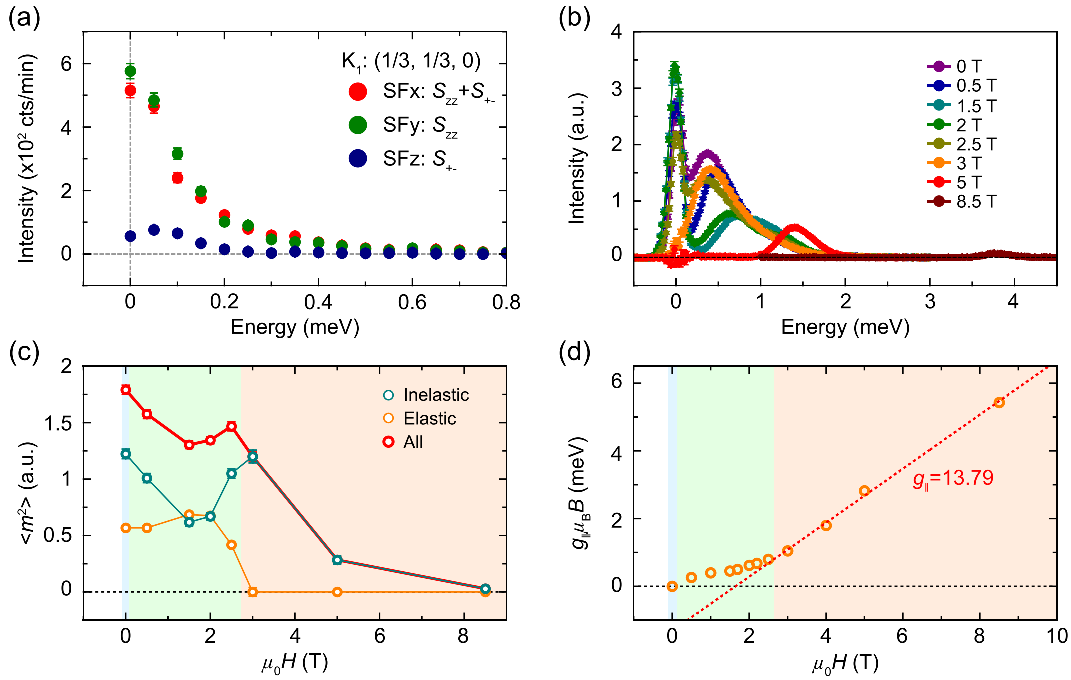

Fig. 4. (Color online) Polarized neutron scattering data and the field dependence of the spin excitations. (a) Energy scans at K_1, 0 T and 1.7 K in all the three spin-flip (SF) channels which correspond to different excitation components (Supplementary materials). The tiny peak in SFz channel may come from the leakage of non-spin-flip channel. (b) Energy dependence of the scattering function integrated through the whole Brillouin zone ($-0.5 < L < 0.5$) in different external fields at 0.12 K. (c) Field dependence of the total local moment $\langle m^2 \rangle$ (All) and the separated elastic and inelastic contributions (Supplementary materials). (d) The external field term, $g_{\parallel}\mu_B B$, used during the LSW calculation versus the experimentally applied field values, $\mu_0 H$. The dashed red line denotes the linear fitting of the data points in Phase III, which gives the g-factor along the z direction.

nearly polarized state (Phase III), making the magnetic state more classical. Meanwhile, the spin gap increases with field and the quantum excitations are progressively suppressed (Fig. 3c–e).

2.4. Spin wave calculation

To quantitatively describe the field tuned quantum effects, we utilize mean-field approach to solve TFIM by introducing the virtual y axis, which lies in the structural ab plane but does not correspond to any real direction, and can even vary from site to site. In this semi-classical picture, the pseudo-spin has a uniform size but becomes tilted from the Ising axis to y direction owing to the transverse field. The effective spin structures of the three phases are illustrated in Fig. 1e–g. Since the transverse components of the effective spins, S^x and S^y, transform as multipoles, only the moment projection in the z direction contributes to the magnetic Bragg peak, making the peak intensity at K point vary with longitudinal field (Fig. 2d). Regarding the INS process, measuring S^z moment will flip the multipolar components and trigger coherent spin wave excitations in S_{zz} channel [32,40], consistent with our polarized neutron measurements. Based on this, we use LSW theory through the SPINW program to simulate the quantum excitations of TFIM in longitudinal fields [41]. The Ising interactions and transverse field term are determined by fitting the zero-field spin excitation spectra, which are $J_1^{zz} = 0.54$ meV, $J_2^{zz} = 0.026$ meV, $h_y = 0.62$ meV [23]. We show that the LSW theory can describe the observed quantum excitations throughout the phase diagram (Fig. 3f–j). The field-dependent evolution of the magnetic Bragg peak, spin gap, overall spectra intensity and dispersions are reproduced reasonably well by the LSW theory (Supplementary materials).We note that the simulated magnetic field is slightly smaller than the applied field (Fig. 4d); this is probably due to the collective quantum effect that is not considered in the LSW calculations. More sophisticated calculation such as the renormalized spin wave theory that takes into account the quantum correction to ordered moments may further refine this analysis. A recent quantum Monte-Carlo (QMC) calculations actually suggested slightly larger exchange coupling constants than the LSW theory calculations, but the ratio of J_2/J_1 remains nearly the same, which is not surprising and does not qualitatively change the magnetic structure and phase diagram based on semi-classical calculations [28,42]. When the external field is relatively large, collective quantum effects are largely suppressed and the LSW calculation becomes more accurate. We can extract the effective g-factor of 13.79 from the high field fitting (Fig. 4d), which is close to the reported value determined by magnetization measurement [29].

3. Discussion and conclusion

It has been suggested theoretically that Phase I will melt in a two-step manner through two Berezinskii-Kosterlitz-Thouless (BKT) transitions and the intermediate BKT phase hosts an emergent U(1) symmetry [15–17,28,42]. Furthermore, it is predicted that in the BKT phase the magnetic susceptibility will diverge in the small longitudinal field limit with a unique scaling behavior [16,17]. However, this is not observed in our magnetization measurements (Supplementary materials). A recent work reports susceptibility data and numerical simulation showing BKT behavior between 0.6 and 0.9 T [43] which, however, lies deep into Phase II of our phase diagram. It has been well established that as a quasi-long-range ordered state, the BKT phase is fragile to perturbations and can be easily killed by external field (<0.1 T) as indicated by QMC calculations [44]. Thus, the claimed evidence for BKT physics for the up–down-zero phase and the comparison are then irrelevant. In addition, no divergence of susceptibility was found in Ref. [43] near the zero-field regime. It should be noted that according to QMC simulation [44], the upper BKT transition would involve into a second-order transition in longitudinal field, which is also inconsistent with Ref. [43]. An earlier calculation suggested that a new magnetic peak at M point should appear at high temperatures owing to proliferated vortex-antivortex pairs [42], which is not observed in our neutron scattering measurements (Supplementary materials).

To summarize, we have performed neutron scattering measurements on the intrinsic quantum Ising magnet $TmMgGaO_4$ in longitudinal fields. In weak field, the zero-field three-sublattice order is replaced by an intermediate quasi-plateau phase, in which both the static moments and spin gap behave in a non-monotonic manner as a function of external field. In high field, the system is driven into the field-induced polarized state. Through a semi-classical analysis, we show that the observed magnetic order and the associated quantum excitations can be well described by TFIM throughout the phase diagram with the subtle competition among quantum fluctuations, frustrated Ising interactions, and thermal fluctuations. Our results demonstrate that $TmMgGaO_4$, as a rare experimental realization of 2D TFIM, is a remarkable platform to illustrate the interplay between quantum and classical interactions, and that the associated quantum states can be manipulated through external fields in a highly controlled manner.

Conflict of interest

The authors declare that they have no conflict of interest.

Acknowledgments

This work was supported by the Innovation Program of Shanghai Municipal Education Commission (2017–01-07–00-07-E0001 8), the National Key R&D Program of the MOST of China (2016YFA0300203, 2016YFA0300500, 2016YFA0301001, and 2018YFE0103200), the National Natural Science Foundation of China (11874119), Shanghai Municipal Science and Technology Major Project (2019SHZDZX04), and the Hong Kong Research Grants Council (17303819 and 17306520). Y.F. and X.T. were supported by the National Natural Science Foundation of China (11875265), the Scientific Instrument Developing Project of the Chinese Academy of Sciences (3He based neutron polarization devices), the Institute of High Energy Physics, and the Chinese Academy of Sciences. The datasets for the inelastic neutron scattering experiment on the time-of-flight LET spectrometer are available from the ISIS facility, Rutherford Appleton Laboratory data portal (10.5286/ISIS.E.RB1910127). The datasets for the polarized neutron scattering experiment on the cold triple-axis ThALES spectrometer are available from the Institute Laue-Langevin data portal (https://doi.ill.fr/10.5291/ILL-DATA.4–05-755). The neutron experiment at the Materials and Life Science Experimental Facility of the J-PARC was performed under a user program (Proposal No. 2019A0116). All other data that support the plots within this paper and other findings of this study are available from the corresponding authors upon reasonable request.

Author contributions

Jun Zhao and Gang Chen planned the project. Yayuan Qin, Yao Shen, and Shoudong Shen synthesized the sample. Yao Shen and Xiaowen Zhang characterized the sample. Yayuan Qin, Yao Shen, Hongliang Wo, Yu Feng, Gaofeng Ding, Yiqing Gu, Qisi Wang, Helen C. Walker, Xin Tong and Jun Zhao carried out the neutron experiments with experimental assistance from Robert Bewley, Jianhui Xu, Martin Boehm, Paul Steffens, Seiko Ohira-Kawamura, Naoki Murai, and Astrid Schneidewind. Jun Zhao, Yayuan Qin and Yao Shen analyzed the data. Changle Liu, Yonghao Gao, and Gang Chen provided the theoretical support and analysis. Jun Zhao, Gang Chen, Yao Shen, Changle Liu, and Yonghao Gao wrote the paper. All authors provided comments on the paper. Yayuan Qin and Yao Shen contributed equally to this work.

Appendix A. Supplementary materials

Supplementary materials to this article can be found online at https://doi.org/10.1016/j.scib.2021.08.012.

References

[1] Onsager L. Crystal statistics. I. A two-dimensional model with an order-disorder transition. Phys Rev 1994;65:117.
[2] Ramirez A. Strongly geometrically frustrated magnets. Annu Rev Mater Sci 1994;24:453.
[3] Sachdev S. Quantum phase transitions. Cambridge, England: Cambridge University Press; 2011.
[4] Moessner R, Sondhi SL, Chandra P. Two-dimensional periodic frustrated Ising models in a transverse field. Phys Rev Lett 2000;84:4457.
[5] Savary L, Balents L. Disorder-induced quantum spin liquid in spin ice pyrochlores. Phys Rev Lett 2017;118:087203.
[6] Mikeska H-J, Steiner M. Solitary excitations in one-dimensional magnets. Adv Phys 1991;40:191.
[7] Bitko D, Rosenbaum TF, Aeppli G. Quantum critical behavior for a model magnet. Phys Rev Lett 1996;77:940.
[8] Coldea R, Tennant DA, Wheeler EM, et al. Quantum criticality in an Ising chain: Experimental evidence for emergent E_8 symmetry. Science 2010;327:177.
[9] Faure Q, Takayoshi S, Petit S, et al. Topological quantum phase transition in the Ising-like antiferromagnetic spin chain $BaCo_2V_2O_8$. Nat Phys 2018;14:716.
[10] Matsuda M, Onishi H, Okutani A, et al. Magnetic structure and dispersion relation of the S=1/2 quasi-one-dimensional Ising-like antiferromagnet $BaCo_2V_2O_8$ in a transverse magnetic field. Phy Rev B 2017;96:024439.
[11] Zou H, Cui Y, Wang X, et al. Exceptional E_8 symmetry in spin dynamics of quasi-one-dimensional antiferromagnet $BaCo_2V_2O_8$. arXiv: 2005.13302, 2020.
[12] Wang Z, Wu J, Yang W, et al. Experimental observation of Bethe strings. Nature 2018;554:219.
[13] Wang Z, Lorenz T, Gorbunov DI, et al. Quantum criticality of an Ising-like spin-1/2 antiferromagnetic chain in a transverse magnetic field. Phys Rev Lett 2018;120:207205.
[14] Moessner R, Sondhi SL. Ising models of quantum frustration. Phys Rev B 2001;63:224401.
[15] Isakov SV, Moessner R. Interplay of quantum and thermal fluctuations in a frustrated magnet. Phys Rev B 2003;68:104409.
[16] Damle K. Melting of three-sublattice order in easy-axis antiferromagnets on triangular and Kagome lattices. Phys Rev Lett 2015;115:127204.
[17] Biswas S, Damle K. Singular ferromagnetic susceptibility of the transverse-field Ising antiferromagnet on the triangular lattice. Phys Rev B 2018;97:085114.
[18] Wang Y, Humeniuk S, Wan Y. Tuning the two-step melting of magnetic order in a dipolar Kagome spin ice by quantum fluctuations. Phys Rev B 2020;101:134414.
[19] Wang Y, Cooper BR. Collective excitations and magnetic ordering in materials with singlet crystal-field ground state. Phys Rev 1968;172:539–51.
[20] Chen G. Intrinsic transverse field in frustrated quantum Ising magnets: physical origin and quantum effects. Phys Rev Res 2019;1:033141.
[21] Dun Z, Bai X, Paddison JAM, et al. Quantum versus classical spin fragmentation in dipolar Kagome ice $Ho_3Mg_2Sb_3O_{14}$. Phys Rev X 2020;10:031069.
[22] Cevallos AF, Stolze K, Kong T, et al. Anisotropic magnetic properties of the triangular plane lattice material $TmMgGaO_4$. Mater Res Bull 2018;105:154–8.
[23] Shen Y, Liu C, Qin Y, et al. Intertwined dipolar and multipolar order in the triangular-lattice magnet $TmMgGaO_4$. Nat Commun 2019;10:4530.
[24] Balents L. Spin liquids in frustrated magnets. Nature 2010;464:199.
[25] Zhou Y, Kanoda K, Ng T-K. Quantum spin liquid states. Rev Mod Phys 2017;89:025003.
[26] Shen Y, Li Y-D, Wo H, et al. Evidence for a spinon Fermi surface in a triangular-lattice quantum-spin-liquid candidate. Nature 2016;540:559.
[27] Shen T, Li Y-D, Walker HC, et al. Fractionalized excitations in the partially magnetized spin liquid candidate $YbMgGaO_4$. Nat Commun 2018;9:4138.
[28] Liu C, Huang C-J, Chen G. Intrinsic quantum Ising model on a triangular lattice magnet $TmMgGaO_4$. Phys Rev Research 2020;2:043013.
[29] Li Y, Bachus S, Deng H, et al. Partial up-up-down order with the continuously distributed order parameter in the triangular antiferromagnet $TmMgGaO_4$. Phys Rev X 2020;10:011007.
[30] Santini P, Carretta S, Amoretti G, et al. Multipolar interactions in f-electron systems: the paradigm of actinide dioxides. Rev Mod Phys 2009;81:807–63.
[31] Alistair CS, Gerd F, Dmytro IS. Multipolar phases and magnetically hidden order: review of the heavy-fermion compound $Ce_{1-x}La_xB_6$. Rep Prog Phys 2016;79:066502.
[32] Liu C, Li Y, Chen G. Selective measurements of intertwined multipolar orders: non-Kramers doublets on a triangular lattice. Phys Rev B 2018;98:045119.
[33] Kadowaki H, Takatsu H, Taniguchi T, et al. Composite spin and quadrupole wave in the ordered phase of $Tb_{2+x}Ti_{2-x}O_{7+y}$. SPIN 2015;5:1540003.

[34] Grenier B, Simonet V, Canals B, et al. Neutron diffraction investigation of the H-T phase diagram above the longitudinal incommensurate phase of $BaCo_2V_2O_8$. Phys Rev B 2015;92:134416.
[35] Schick M, Walker JS, Wortis M. Phase diagram of the triangular Ising model: renormalization-group calculation with application to adsorbed monolayers. Phys Rev B 1977;16:2205.
[36] Miyashita S. Magnetic properties of Ising-like Heisenberg antiferromagnets on the triangular lattice. J Phys Soc Jpn 1986;55:3605.
[37] Honecker A. A comparative study of the magnetization process of two-dimensional antiferromagnets. J Phys: Condens Matter 1999;11:4697.
[38] Sellmann D, Zhang X, Eggert S. Phase diagram of the antiferromagnetic *XXZ* model on the triangular lattice. Phys Rev B 2015;91:081104.
[39] Yamamoto D, Marmorini G, Danshita I. Quantum phase diagram of the triangular-lattice *XXZ* model in a magnetic field. Phys Rev Lett 2014;112:127203.
[40] Li Y, Chen G. Symmetry enriched U(1) topological orders for dipole-octupole doublets on a pyrochlore lattice. Phys Rev B 2017;95:041106.
[41] Toth S, Lake B. Linear spin wave theory for single-*Q* incommensurate magnetic structures. J Phys: Condens Matter 2015;27:166002.
[42] Li H, Liao Y-D, Chen B, et al. Kosterlitz-Thouless melting of magnetic order in the triangular quantum Ising material $TmMgGaO_4$. Nat Commun 2020;11:1111.
[43] Hu Z, Ma Z, Liao Y-D, et al. Evidence of the Berezinskii-Kosterlitz-Thouless phase in a frustrated magnet. Nat Commun 2020;11:5631.
[44] Liao YD, Li H, Yan Z, et al. Phase diagram of the quantum Ising model on a triangular lattice under external field. Phys Rev B 2021;103:104416.

Yayuan Qin received her Bachelor degree of Science from Central South University. Now she is a Ph.D. candidate at Department of Physics, Fudan University. Her research mainly focuses on various strong correlated systems, including unconventional superconductors and frustrated systems.

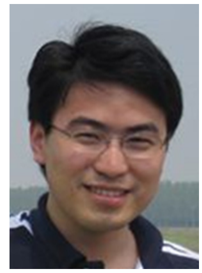

Gang Chen is a faculty at Department of Physics, University of Hong Kong. He received the B.S. degree from University of Science and Technology of China in 2004, and Ph.D. degree from University of California, Santa Barbara in 2010. He has ever worked as a post-doctoral fellow in University of Colorado Boulder and University of Toronto. Then, he moved to Fudan University as a professor in early 2015 and then University of Hong Kong in 2018. His current research interest includes theoretical study on various condensed matters systems, including quantum materials, topological phases, and strongly correlated systems.

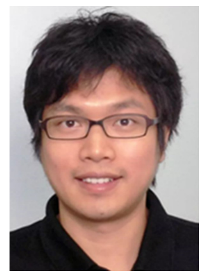

Jun Zhao received the B.S. degree from Tsinghua University in 2002, and the M.S. degree from Institute of Physics, Chinese Academy of Sciences in 2005. He received his Ph.D. degree in Physics from the University of Tennessee, Knoxville in 2010. Then, he worked at UC Berkeley as a Miller Fellow. He is currently the Xie Xide Junior Chair Professor at Department of Physics, Fudan University, where he has been a faculty member since 2012. His research mainly focuses on using various neutron scattering techniques to study the phase transitions and spin dynamics of strongly correlated systems, including unconventional superconductors and quantum magnets.